The Journal of Immunology

RESEARCH ARTICLE | APRIL 17 2023

Borrelia burgdorferi Engages Mammalian Type I IFN Responses via the cGAS–STING Pathway

Lauren C. Farris; ... et. al

J Immunol ji2200354.
https://doi.org/10.4049/jimmunol.2200354

Borrelia burgdorferi Engages Mammalian Type I IFN Responses via the cGAS–STING Pathway

Lauren C. Farris,* Sylvia Torres-Odio,* L. Garry Adams,† A. Phillip West,* and Jenny A. Hyde*

***Borrelia burgdorferi*, the etiologic agent of Lyme disease, is a spirochete that modulates numerous host pathways to cause a chronic, multisystem inflammatory disease in humans. *B. burgdorferi* infection can lead to Lyme carditis, neurologic complications, and arthritis because of the ability of specific borrelial strains to disseminate, invade, and drive inflammation. *B. burgdorferi* elicits type I IFN (IFN-I) responses in mammalian cells and tissues that are associated with the development of severe arthritis or other Lyme-related complications. However, the innate immune sensors and signaling pathways controlling IFN-I induction remain unclear. In this study, we examined whether intracellular nucleic acid sensing is required for the induction of IFN-I to *B. burgdorferi*. Using fluorescence microscopy, we show that *B. burgdorferi* associates with mouse and human cells in culture, and we document that internalized spirochetes colocalize with the pattern recognition receptor cyclic GMP-AMP synthase (cGAS). Moreover, we report that IFN-I responses in mouse macrophages and murine embryonic fibroblasts are significantly attenuated in the absence of cGAS or its adaptor stimulator of IFN genes (STING), which function to sense and respond to intracellular DNA. Longitudinal in vivo tracking of bioluminescent *B. burgdorferi* revealed similar dissemination kinetics and borrelial load in C57BL/6J wild-type, cGAS-deficient, or STING-deficient mice. However, infection-associated tibiotarsal joint pathology and inflammation were modestly reduced in cGAS-deficient compared with wild-type mice. Collectively, these results indicate that the cGAS–STING pathway is a critical mediator of mammalian IFN-I signaling and innate immune responses to *B. burgdorferi*. *The Journal of Immunology*, 2023, 210: 1–10.**

Lyme disease results from infection with the spirochetal bacterium *Borrelia burgdorferi* and presents as a multisystemic inflammatory disease causing debilitating morbidity as a result of fatigue, malaise, severe arthritis, and cardiac and neurologic complications (1–4). It is the most common tick-borne disease in the United States and is a significant public health concern, with the Centers for Disease Control and Infection reporting 39,000 cases per year, but insurance reports indicating a prevalence of greater than 470,000 cases per year (5–7). Antibiotic treatment is highly effective when administered shortly after the tick bite, yet antibiotic efficacy declines as the borrelial infection progresses (8, 9). Lyme disease occurs in stages of localized, disseminated, and chronic infection as the extracellular pathogen spreads from the site of the tick bite to secondary tissues, including the joints, heart, and CNS, causing Lyme arthritis, carditis, and neuroborreliosis, respectively (1–3, 8). The development of arthritis, a characteristic symptom of late Lyme disease in North America, is associated with a robust innate immune response that includes induction of type I IFN (IFN-I) cytokines (10–12).

B. burgdorferi elicits a robust innate immune response, resulting in the secretion of proinflammatory cytokines and chemokines (13–20). In addition, *B. burgdorferi* triggers IFN-I responses in a wide array of human cells, mouse cells, and infected tissues (11–13, 19, 21–28). Evidence suggests that innate IFN-I signaling plays key roles in several aspects of *B. burgdorferi* pathology (29–33). Notably, IFN-I and resulting IFN-stimulated gene (ISG) signatures are linked to the development of more severe arthritis in experimental models and also correlate with lingering neurocognitive symptoms of Lyme disease (12, 30, 32, 34). In addition, a recent study from Lochhead and colleagues (35) observed that a robust IFN gene signature correlates with decreased expression of tissue-repair genes in synovial lesion biopsies from patients with postinfectious, *B. burgdorferi*–induced Lyme arthritis. It is well appreciated that innate immune sensing of the abundant *B. burgdorferi* lipoproteins via TLR2 triggers production of proinflammatory cytokines and chemokines in vitro and in vivo (14, 36–38). However, lipoprotein binding to TLR2 is not a robust inducer of IFN-I responses in most mouse and human cell types (39, 40). Studies using human cells have implicated nucleic acid–sensing TLRs (TLR7, 8, and 9) as regulators of IFN-I induction in human immune cells challenged with *B. burgdorferi* in vitro (13, 18, 19). In contrast, other reports have shown that *B. burgdorferi* can engage IFN-I responses in nonphagocytic fibroblasts and endothelial cells, which do not express a full complement of TLRs (25, 41). Moreover, *B. burgdorferi*–related ISG induction in murine macrophages is independent of the two primary TLR adaptor proteins MyD88 and TRIF (22, 23). Thus, TLR-mediated sensing of *B. burgdorferi* pathogen-associated molecular patterns does not appear to be the

*Department of Microbial Pathogenesis and Immunology, School of Medicine, Texas A&M University, Bryan, TX; and †Department of Veterinary Pathobiology, School of Veterinary Medicine and Biomedical Sciences, Texas A&M University, College Station, TX

ORCIDs: 0000-0002-7246-1602 (L.G.A.); 0000-0003-2884-6895 (A.P.W.); 0000-0001-9442-9980 (J.A.H.).

Received for publication May 16, 2022. Accepted for publication March 23, 2023.

This work was supported by the National Institute of Allergy and Infectious Diseases, National Institutes of Health Grant R21AI153879 (to A.P.W. and J.A.H.) and National Heart, Lung, and Blood Institute, National Institutes of Health Grants R01HL148153 (to A.P.W.) and F31HL160141 (to S.T.-O.).

Address correspondence and reprint requests to Dr. A. Phillip West and Dr. Jenny A. Hyde, Texas A&M University School of Medicine, 8447 Riverside Parkway, MREB 1 3012, Bryan, TX 77807. E-mail addresses: awest@tamu.edu (A.P.W.) and jhyde@tamu.edu (J.A.H.)

The online version of this article contains supplemental material.

Abbreviations used in this article: BMDM, bone marrow–derived macrophage; cGAS, cyclic GMP-AMP synthase; *Gbp2*, guanylate-binding protein 2; HA, hemagglutinin; HFF, human foreskin fibroblast; iBMDM, immortalized mouse bone marrow–derived macrophage; IFIT1, IFN-induced protein with tetratricopeptide repeats 1; IFNAR, type I IFN receptor; IFN-I, type I IFN; IRF3, IFN regulatory factor 3; ISD, immunostimulatory DNA; ISG, IFN-stimulated gene; KO, knockout; MAVS, mitochondrial antiviral signaling; MEF, mouse embryonic fibroblast; MOI, multiplicity of infection; mtDNA, mitochondrial DNA; OspA, outer surface protein A; qRT-PCR, quantitative RT-PCR; STING, stimulator of IFN genes; TBK1, Tank-binding kinase 1; WT, wild-type.

predominant trigger of IFN-I responses in mammalian cells during infection.

Innate immune pathways that sense cytosolic nucleic acids, such as the RIG-I–like receptor–mitochondrial antiviral signaling (MAVS) or cyclic GMP-AMP synthase (cGAS)-stimulator of IFN genes (STING) pathway, have emerged as key regulators of IFN-I production in both immune and nonimmune cells (42–49). cGAS is an intracellular DNA sensor that localizes to the mammalian cell cytoplasm and nucleus. Upon binding intracellular pathogen DNA, micronuclei, or mitochondrial DNA (mtDNA), cGAS generates the noncanonical cyclic dinucleotide, 2′3′-cyclic guanosine monophosphate-adenosine monophosphate, which binds STING. This results in the recruitment and activation of Tank-binding kinase 1 (TBK1), leading to the phosphorylation of IFN regulatory factor 3 (IRF3) for the induction of IFN-Is (IFNα, β) and ISGs (42–44). Although initially identified as an antiviral host defense pathway, the cGAS–STING pathway is also critical for induction of robust IFN-I responses to intracellular bacteria, such as *Mycobacterium tuberculosis* and *Listeria monocytogenes* (45, 50, 51). Moreover, recent work has shown that the cGAS–STING pathway is essential for IFN-I production in response to multiple extracellular pathogens, including *Pseudomonas aeruginosa*, *Klebsiella pneumoniae*, and *Staphylococcus aureus* (52, 53). *B. burgdorferi*, predominantly an extracellular pathogen, is readily taken up by phagocytic cells and associates with endothelial cells and fibroblasts, which are key sources of IFN-I in the Lyme disease joint (54–62). *B. burgdorferi* also produces cyclic dinucleotides c-di-GMP and c-di-AMP, which can directly engage STING (63–66). Thus, there are several potential routes by which *B. burgdorferi* infection could trigger the cGAS–STING–IFN-I pathway.

In this study, we tested the hypothesis that *B. burgdorferi* infection induces IFN-I through the cGAS–STING pathway. We exposed phagocytic and nonphagocytic cells lacking various components of the cytosolic nucleic acid–sensing machinery to viable and sonicated *B. burgdorferi* and evaluated IFN-I and ISG expression after exposure. We also assessed the degree of association of *B. burgdorferi* with cultured fibroblasts and examined colocalization of cGAS with intracellular spirochetes. Furthermore, we performed an infectivity study with bioluminescent *B. burgdorferi* in mice deficient in cGAS or STING to assess borrelial load by in vivo imaging and joint inflammation using histopathology. Our results reveal that *B. burgdorferi* engages IFN-I responses in a cGAS-STING–dependent manner without significantly altering infection kinetics or borrelial load in tissues.

Materials and Methods

Mouse and B. burgdorferi *strains*

C57BL/6J (strain 000664), cGAS-deficient (cGAS knockout [$cGAS^{KO}$], strain 026554), STING-deficient ($STING^{KO}$, strain 017537), IFN-I receptor (IFNAR)-deficient ($IFNAR^{KO}$, strain 028288), and MAVS-deficient ($MAVS^{KO}$, strain 008634) mice were obtained from the Jackson Laboratory. $MAVS^{KO}$ mice were backcrossed to C57BL/6J mice for 10 generations before generation of primary cell lines. Mice were group housed in humidity-controlled environments maintained at 22°C on 12-h light–dark cycles (600–1800 h). Food and water were available ad libitum. All animal experiments were conducted in accordance with guidelines established by Department of Health and Human Services *Guide for the Care and Use of Laboratory Animals* and the Texas A&M University Institutional Animal Care and Use Committee.

Low-passage *B. burgdorferi* strains B31-A3 and ML23 pBBE22*luc* were cultured in BSK-II medium with 6% normal rabbit serum (Pel-Freeze Biologicals, Rogers, AR) and grown to midlog phase at 37°C at 5% CO_2 (67–71). ML23 pBBE22*luc* cultures were supplemented with 300 μg/ml kanamycin.

Cell culture and B. burgdorferi *infection*

Primary mouse embryonic fibroblasts (MEFs) were generated from WT, $cGAS^{KO}$, $STING^{KO}$, $IFNAR^{KO}$, and $MAVS^{KO}$ embryonic day 12.5 to 14.5 embryos. Cells were grown in DMEM (D5756; Millipore Sigma) containing 10% low endotoxin FBS (97068-085; VWR) and cultured for no more than four passages before experiments. SV40 immortalized $cGAS^{KO}$ MEFs reconstituted with hemagglutinin (HA)-tagged mouse cGAS were previously reported (72). Primary bone marrow–derived macrophages (BMDMs) were generated as described previously (73). In brief, bone marrow cells were collected from the femur and tibia of mice and differentiated into macrophages in DMEM containing 10% low endotoxin FBS and 20% (v/v) conditioned media harvested from L929 cells (CCL-1; ATCC). Cells were plated in petri plates and maintained in L929-conditioned media for 7 d. The day before experiments, macrophages were plated in tissue culture plates and maintained in 5% L929. To generate immortalized mouse macrophages (iBMDMs), we infected BMDMs with J2 recombinant retrovirus (encoding v-myc and v-raf oncogenes) as described previously (74). iBMDMs were passaged for 3–6 mo and were slowly weaned off of L929 conditioned media until they stabilized into cell lines. Human foreskin fibroblasts (HFFs; SCRC-1041; ATCC) were immortalized using a human telomerase-expressing retrovirus (pWZL-Blast-Flag-HA-hTERT, 22396; Addgene).

Bacteria were prepared as previously described (61) with the following exceptions. *B. burgdorferi* was grown to midexponential phase, centrifuged at 6600 × *g* for 8 min, washed twice in PBS, and resuspended in DMEM (D5796; Millipore Sigma) with 10% FBS (97068-085; VWR). Spirochetes were enumerated using dark-field microscopy and diluted to the appropriate multiplicity of infection (MOI). Where indicated, plates were spun after the addition of bacteria to mammalian cells for 5 min at 300 × *g*. Small molecule inhibitors were added to MEFs 1 h before *B. burgdorferi* infection. cGAS inhibitor RU.521 (HY-114180; MedChemExpress) and STING inhibitor H-151 (HY-112693; MedChemExpress) were added at 10 and 0.5 mM, respectively (75, 76). MEFs or BMDMs were transfected with 2 μg/ml IFN Stimulatory DNA (tlrl-isdn; InvivoGen) complexed with Lipofectamine 2000 (11668019; ThermoFisher) in Opti-MEM media (11058021; Life Technologies) for 5–20 min (73).

Quantitative PCR and RT-PCR

RNA was isolated from mammalian cells using the Quick-RNA Micro Prep Kit (R1051; Zymo Research) according to the manufacturer's instructions. Between 300 and 500 ng of RNA was standardized across samples from each experiment and converted to cDNA with the qScript cDNA Synthesis Kit (95047; QuantaBio). Quantitative PCR was performed on cDNA using the PerfecTa SYBR Green FastMix (95072; QuantaBio) and primers listed in Table I. Each biological sample was assayed in triplicate. Relative expression was determined for each triplicate after normalization against a housekeeping gene (*Bactin* or *Gapdh*) using the $2^{-\Delta\Delta CT}$ method. DNA contamination of RNA samples was evaluated in a single, no reverse transcriptase reaction for each primer set.

Immunoblotting

Protein was collected from cells lysed in 1% Nonidet P-40 buffer (50 mM Tris [pH 7.5], 0.15 M NaCl, 1 mM EDTA, 1% Nonidet P-40, and 10% glycerol) supplemented with protease inhibitor (04693159001; Roche) and spun for 10 min at 17,000 × *g* at 4°C. The supernatant was collected and stored at −80°C. Protein lysates were quantified using the micro-BCA assay (23235; ThermoFisher Scientific, Waltham, MA). Immunoblotting was performed as described by Torres-Odio et al. (77). In brief, between 20 and 30 mg protein was run on 10–20% SDS-PAGE gradient gels and transferred onto 0.22 μM polyvinylidene difluoride membranes (1620177; Bio-Rad). After air-drying to return to a hydrophobic state, membranes were incubated in primary Abs (Table II) at 4°C overnight in 1× PBS containing 1% casein, HRP-conjugated secondary Ab at room temperature for 1 h, and then developed with Luminata Crescendo Western HRP Substrate (WBLUR0500; Millipore).

Immunofluorescence microscopy

Cells were seeded on 12- or 18-mm sterile coverslips, allowed to adhere overnight, and infected as described earlier. At the conclusion of infection, cells were washed with DMEM and then 1× PBS, fixed with 4% paraformaldehyde for 15 min at room temperature, and washed twice with 1× PBS for 5 min each. Cells were permeabilized with 0.1% Triton X-100 in PBS for 5 min at room temperature, washed twice with 1× PBS, and blocked for 30 min in PBS containing 5% FBS. Each coverslip was stained with primary (Table II) and secondary Abs for 1 h each. Cells were washed in 1× PBS with 5% FBS three times after each stain for 5 min each. After the last wash, cells were incubated with CellMask Green (H32714; Invitrogen) for 30 min at 1:500 dilution in 1× PBS. Then, cells were washed two times more for 5 min each with 1× PBS. After the last wash, cells were incubated with DAPI (62247; ThermoFisher Scientific) for 2 min at 1:2000 dilution in 1× PBS. Cells were washed two times more for 5 min each with 1× PBS, and coverslips were mounted with ProLong Diamond Antifade Mountant (P36961; Invitrogen) and allowed to dry overnight.

Images in Figs. 2E and 3A were captured with a LSM 780 confocal microscope (Zeiss) with a 63× oil-immersed objective. Z-stack images were processed using Zeiss ZEN 3.3 software. Images in Fig. 3F and Supplemental Fig. 1A were taken with an ECLIPSE Ti2 microscope (Nikon) with a 60× oil-immersed or 40× dry objective, respectively, and NIS-Elements AR 5.21.02 software. Images in Fig. 3F were imported into Huygens Essential software (v21.4.0) and deconvolved using the "aggressive" profile in the Deconvolution Express application. Images in Supplemental Fig. 1E were captured with an Olympus FV3000 confocal laser scanning microscope and a 60× oil-immersed objective.

For quantification of *B. burgdorferi* associated with cultured MEF and HFF cells (Supplemental Fig. 1A), tiled images from infected cells at 24 h postinfection were taken with 40× objective. From each field, the number of cells with more than one *B. burgdorferi* present in the cell area, defined by positive CellMask staining, was annotated. *B. burgdorferi*–positive cells were divided by the total number of cells per field, defined by counting DAPI-positive nuclei, and multiplied by 100 to calculate the percentage of cells associated with *B. burgdorferi*. Four fields for each cell line 6 and 24 h postinfection were quantified from duplicate biological samples, and the average of each cell line across replicates and fields was plotted.

Mouse infection with B. burgdorferi *with in vivo bioluminescent imaging*

Bioluminescent images of mice were collected as previously described (70, 78). Groups of five WT, five cGAS^{KO}, and five STING^{KO} male mice 6–11 wk old were s.c. injected with 100 μl of 10^5 ML23 pBBE22*luc.* Before imaging, 5 mg of D-luciferin (Goldbio, St. Louis, MO) was dissolved in PBS and administered to all except one mouse per group via i.p. injection and anesthetized with isoflurane for imaging. Mice were imaged at 1 h and 1, 4, 7, 10, 14, 21, and 28 d postinfection (dpi) using the Perkin Elmer IVIS Spectrum live imaging system. Bioluminescence from treated mice was normalized to the untreated mouse from each group. At 28 dpi, inguinal lymph nodes and skin flanks were collected and transferred to BSKII with 6% normal rabbit serum for outgrowth assays.

Histopathology

Samples of joints and hearts were collected from each mouse after euthanasia at 28 and 35 dpi, fixed by immersion in 10% neutral-buffered formalin at room temperature for 48 h, and stored in 70% ethanol before embedding in paraffin, sectioning at 5–6 μm, and staining with H&E by AML Laboratories (Jacksonville, FL). The tissue sections were examined using bright-field microscopy in a blinded manner by a board-certified anatomic veterinary pathologist and ordinally scored for the degree of mononuclear infiltration. A score of 1 represented minimal infiltration (<5 cells/400× field) and increased to 4 for abundant infiltration (>30 cells/400× field). Tissue sections were also scored for distribution of mononuclear inflammatory cells as focal (1), multifocal (2), or diffuse (3).

Statistical analyses

Statistical analysis was performed in GraphPad Prism (GraphPad Software, La Jolla, CA). Statistical significance was determined by $p \leq 0.05$. Specific tests are detailed in the figure legends. Error bars in figures represent SEM based on the combined triplicate biological samples for all cell culture studies. All cell culture–based results (Figs. 1, 2, 3, Supplemental Figs. 1, 2) are representative of at least three independent experiments. Four biological replicates were used in in vivo bioluminescence imaging (Fig. 4) to determine statistical significance.

Results

Viable B. burgdorferi *elicits a robust IFN-I response in mouse macrophages and fibroblasts*

We first evaluated the ability of iBMDMs and MEFs derived from C57BL/6J mice to upregulate ISG and inflammatory cytokine transcripts when coincubated with viable or sonicated *B. burgdorferi* B31-A3 at an MOI of 20 (Fig. 1). Consistent with earlier reports (19, 60), both viable and sonicated B31-A3 were able to induce IFN-β (*Ifnb1*) and ISGs (*Cxcl10* and guanylate-binding protein 2 [*Gbp2*]), as well as proinflammatory cytokine IL-6 (*Il6*) expression, in iBMDMs (Fig. 1A, 1B). Viable *B. burgdorferi* more potently induced ISGs and *Il6*, inducing expression levels 4- to 10-fold higher than sonicated bacteria (Table I). Likewise, we found that *B. burgdorferi* elicited ISGs and TNF-α (*Tnfa*) in primary MEFs, with live spirochetes triggering more robust responses

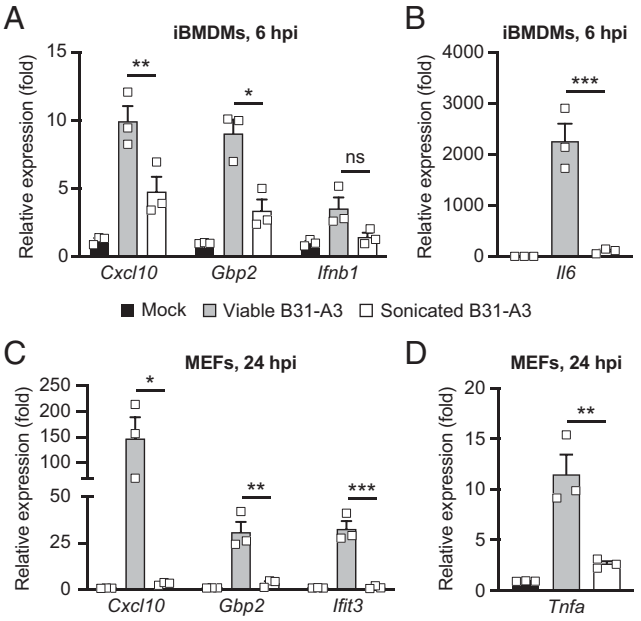

FIGURE 1. Viable *B. burgdorferi* induce robust proinflammatory and IFN-I responses in mouse macrophages and fibroblasts. iBMDMs or MEFs were cocultured with viable or sonicated *B. burgdorferi* strain B31-A3 at an MOI of 20. (**A**) Fold changes in iBMDM transcripts encoding ISGs (*Cxcl10* and *Gbp2*), *Ifnb1*, or (**B**) the proinflammatory cytokine *Il6* were analyzed by qRT-PCR after 6 h of coculture. (**C**) Fold changes in MEF transcripts encoding ISGs (*Cxcl10*, *Gbp2*, and *Ifit3*) and the (**D**) inflammatory cytokine *Tnfa* were analyzed by qRT-PCR after 24 h of coculture. Error bars represent ± SEM of biological triplicate samples. Significance was determined by one-way ANOVA Tukey post hoc for all panels. ***$p < 0.001$, **$p < 0.01$, *$p < 0.05$. ns, not significant.

compared with sonicated bacteria (Fig. 1C, 1D and Table II). Collectively, these data indicate that live *B. burgdorferi* engages robust IFN-I–associated ISG expression in both BMDMs and nonphagocytic MEFs, which lack a full repertoire of TLRs and other pattern recognition receptors (41).

B. burgdorferi *engages the cGAS–STING pathway to induce IFN-I responses in murine macrophages*

Lipoprotein-rich *B. burgdorferi* predominately engage TLR2 but can also trigger other TLRs to induce inflammatory cytokines and IFNs (18, 19, 24, 36). However, a role for cytosolic DNA sensing in the innate immune response to *B. burgdorferi* remains unknown. To examine this directly, we cocultured primary BMDMs from wild-type (WT), cGAS^{KO}, or STING^{KO} mice on a C57BL/6J background with *B. burgdorferi* B31-A3 and assessed ISG and cytokine transcript induction by quantitative RT-PCR (qRT-PCR) (Fig. 2). We first confirmed that cGAS^{KO} BMDMs were hyporesponsive to immunostimulatory DNA (ISD) delivered into the cytosol by transfection (73). As expected, the induction of ISGs *Cxcl10* and *Gbp2* in cGAS^{KO} BMDMs was significantly reduced relative to WT macrophages (Fig. 2A). After 6 h of coculture with B31-A3, the expressions of ISGs *Cxcl10* and *Gbp2*, as well as *Ifnb1* transcripts, were significantly reduced in cGAS^{KO} BMDMs compared with WT (Fig. 2B). In contrast, the levels of *Il-6* and *Tnfa* transcripts were similar in both WT and cGAS$^{-/-}$ BMDMs (Fig. 2C). These results indicate that the cGAS pathway is not a robust inducer of proinflammatory genes in BMDMs exposed to *B. burgdorferi* and are consistent with the notion that TLR2 or other TLRs sense *B. burgdorferi* ligands to engage NF-κB–dependent cytokines. Similar results were obtained from protein analysis of cGAS^{KO} and STING^{KO} macrophages

Table I. Oligonucleotide sequences used in this study

Gene	Forward Primer Sequence	Reverse Primer Sequence
Mouse		
Actb	5′-TTCTTTGCAGCTCCTTCGTT-3′	5′-ATGGAGGGGAATACAGCCC-3′
Cxcl10	5′-CCAAGTGCTGCCGTCATTTTC-3′	5′-GGCTCGCAGGGATGATTTCAA-3′
Gapdh	5′-GACTTCAACAGCAACTCCCAC-3′	5′-TCCACCACCCTGTTGCTGTA-3′
Gbp2	5′-CAGCATAGGAACCATCAACCA-3′	5′-TCTACCCCACTCTGGTCAGG-3′
Ifit3	5′-CAGCATAGGAACCATCAACCA-3′	5′-TCTACCCCACTCTGGTCAGG-3′
Ifnb1	5′-CCCTATGGAGATGACGGAGA-3′	5′-CCCAGTGCTGGAGAAATTGT-3′
Il6	5′-TGATGCACTTGCAGAAAACA-3′	5′-ACCAGAGGAAATTTTCAATAGGC-3′
Tnfa	5′-CCACCACGCTCTTCTGTCTAC-3′	5′-AGGGTCTGGGCCATAGAACT-3′
Human		
GAPDH	5′-AGCCACATCGCTCAGACA-3′	5′-GCCCAATACGACCAAATCC-3′
IFNB1	5′-CTTTCGAAGCCTTTGCTCTG-3′	5′-CAGGAGAGCAATTTGGAGGA-3′
IFI44L	5′-CAATTTAAGCCTGATCTAACCCC-3′	5′-CAGTTGCGCAGATGATTTTC-3′
TNFA	5′-CTGCTGCACTTTGGAGTGAT-3′	5′-AGATGATCTGACTGCCTGGG-3′
B. burgdorferi		
flaB	5′-CAGCTAATGTTGCAAATCTTTTCTCT-3′	5′-TTCCTGTTGAACACCCTCTTGA-3′

9 h after incubation with B31-A3, with notable reductions in ISGs IFN-induced protein with tetratricopeptide repeats 1 (IFIT1) and Z-DNA binding protein 1 in both cGAS^{KO} and STING^{KO} BMDMs (Fig. 2D).

Finally, confocal imaging revealed that *B. burgdorferi* are internalized by BMDMs after a 3-h incubation (Fig. 2E). Ab staining against the outer surface protein A (OspA) of *B. burgdorferi* showed coiled and degraded DAPI-positive spirochetes in the macrophage cytoplasm, as well as punctate, DAPI-negative OspA staining, indicative of bacterial destruction. *B. burgdorferi* OspA also colocalized with the cytosolic autophagy marker p62/Sequestosome-1, suggesting spirochete degradation via macrophage autophagy and/or LC3-associated phagocytosis pathways (79–81). Collectively, these data indicate that *B. burgdorferi* are internalized by murine macrophages and trigger the cGAS–STING–IFN-I signaling axis.

B. burgdorferi *engages the cGAS–STING pathway in fibroblasts*

To broaden our findings beyond murine macrophages, we exposed MEFs and telomerase immortalized HFFs to *B. burgdorferi* B31-A3. We observed that OspA-positive *B. burgdorferi* associated with ∼15% of MEFs (Supplemental Fig. 1A, 1B) and 33% of HFFs (Supplemental Fig. 1C, 1D) after coculture, consistent with a prior study (54). Confocal immunofluorescent imaging with Z-stack reconstitution revealed cell-associated *B. burgdorferi* in the same focal plane with mitochondria (Fig. 3A), suggestive of spirochete internalization. Additional imaging analysis revealed that coiled and degraded spirochetes strongly colocalized with the intracellular autophagy marker p62, further documenting that *B. burgdorferi* can access the fibroblast cytoplasm (Supplemental Fig. 1E). Similar to our results in MEFs, exposure of HFFs to live *B. burgdorferi* increased expression levels of ISGs (*IFI44L*, *IFNB1*) and the proinflammatory cytokine gene *TNFA* (Fig. 3B). Although the synthetic TLR2 ligand PAM3CSK4 (Pam3) induced *TNFA* levels similar to live B31-A3, we did not observe ISG induction, suggesting that *B. burgdorferi* lipoprotein engagement of TLR2 is not responsible for IFN-I responses in HFFs. Taken together, these results demonstrate that *B. burgdorferi* association and internalization within a minority of cultured cells is sufficient to induce robust IFN-I responses.

Table II. Primary Abs used in this study

Ab	Source	Catalogue No.	Dilution
αTubulin	DSHB	12G10	1:5000
cGAS	Cell Signaling	31659	1:1000
HA	Proteintech	51064-2-AP	1:500
HSP60	Santa Cruz	sc-1052	1:5000
IFIT1	Gift from G. Sen at Cleveland Clinic		1:1000
OspA	Capricorn	BOR-018-48310	1:1,000,000
p62	Proteintech	18420-1-AP	1:500
STING	Proteintech	19851-1-AP	1:1000
ZBP1	Adipogen	AG-20B-0010	1:1000

HSP60, heat shock protein 60; ZBP1, Z-DNA binding protein 1.

To next examine whether cGAS contributes to IFN-I responses in fibroblasts exposed to *B. burgdorferi*, we cocultured primary WT and cGAS^{KO} MEFs with B31-A3 and subjected them to qRT-PCR analysis for ISG and proinflammatory transcripts. We first confirmed that cGAS^{KO} MEFs were hyporesponsive to ISD delivered into the cytosol by transfection (Fig. 3C). After coculture with *B. burgdorferi*, we noted that the induction of ISG (*Cxcl10* and *Gbp2*) and *Ifnb1* transcripts was significantly reduced or entirely abrogated in cGAS^{KO} MEFs relative to WT controls (Fig. 3D). Although *Il6* transcripts were similar between *B. burgdorferi*–exposed WT and cGAS^{KO} MEFs, *Tnfa* expression was significantly reduced in the absence of cGAS (Fig. 3E). Immunofluorescence microscopy revealed that *B. burgdorferi* associated with MEFs after a 6-h incubation, similar to results in BMDMs and HFFs (Fig. 3F). Ab staining against the OspA lipoprotein revealed intact, DAPI-positive spirochetes in the MEF cytoplasm, as well as punctate OspA foci that were DAPI negative. Consistent with a role for cGAS in sensing internalized *B. burgdorferi* DNA, we observed colocalization of HA-tagged cGAS with coiled spirochetes staining positive for both OspA and DAPI (Fig. 3F). To further document a requirement for the cGAS–STING pathway in the IFN-I response to *B. burgdorferi*, we employed RU.521, a specific cGAS inhibitor, and H-151, a specific STING inhibitor, to block the pathway during coculture. Both inhibitors were effective at reducing ISG transcripts (*Cxcl10* and *Gbp2*) induced by transfection of ISD (Fig. 3G). MEFs exposed to cGAS and STING inhibitors exhibited reduced ISG expression relative to vehicle-treated MEFs, with no effects on *Tnfa* induction (Fig. 3H). Taken together, these data indicate that *B. burgdorferi* associates with fibroblasts in culture, leading to the cGAS-mediated sensing of borrelial DNA from lysed or damaged spirochetes.

Additional experiments in STING^{KO} MEFs revealed markedly reduced *Gbp2* and *Ifnb1* expression, but little change in proinflammatory cytokine transcripts, after challenge with *B. burgdorferi* (Supplemental Fig. 2A, 2B). MEFs deficient in the IFNAR also exhibited impaired expression of the ISG *Gbp2*, but not cytokine transcripts, suggesting that ISG induction in MEFs is dependent on autocrine and/or paracrine signaling via IFNAR. In contrast, *B. burgdorferi* infection of MAVS protein null MEFs (MAVS^{KO}), which cannot signal in response to intracellular dsRNA, triggered levels of *Gbp2* and *Ifnb1* mirroring WT cells (Supplemental Fig. 2A). This indicates that MEFs cocultured with *B. burgdorferi* respond to DNA, not RNA,

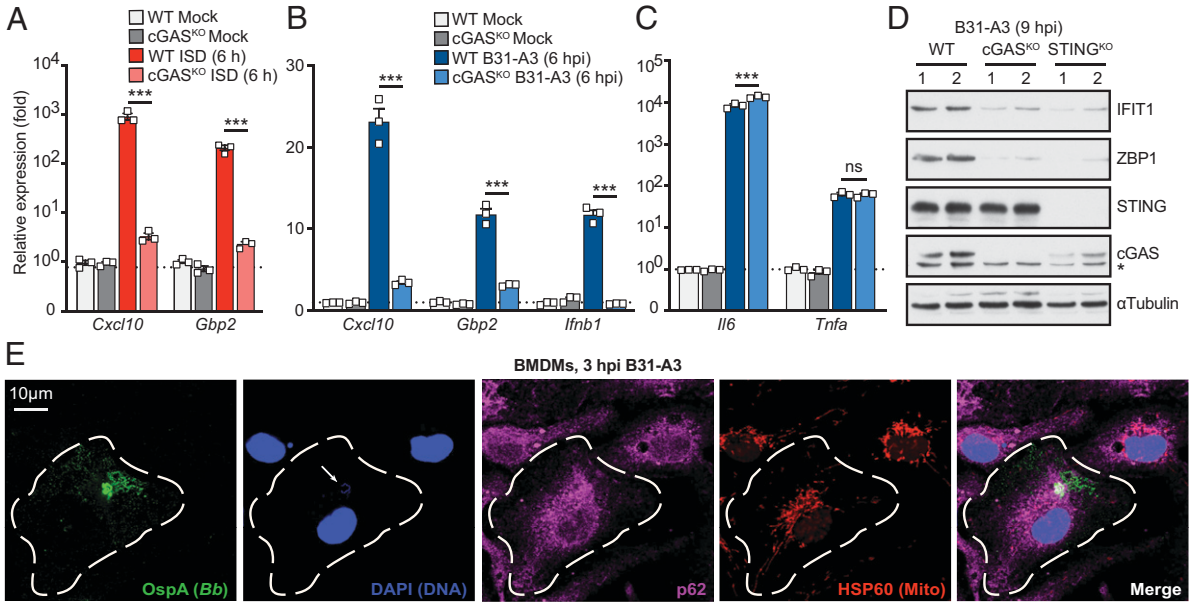

FIGURE 2. cGAS is required for robust ISG expression in mouse macrophages exposed to live *B. burgdorferi*. (**A**) qRT-PCR of ISG transcripts (*Cxcl10*, *Gbp2*) from WT and cGAS^{KO} BMDMs 6 h after transfection with ISD or mock transfected. (**B** and **C**) qRT-PCR of transcripts encoding ISGs (*Cxcl10*, *Gbp2*) and *Ifnb1* (B) or inflammatory cytokines (*Il6* and *Tnfa*) (C) in WT and cGAS^{KO} BMDMs exposed to live *B. burgdorferi* strain B31-A3 for 6 h at MOI of 20. Fold expression values in (A)–(C) are plotted relative to WT mock samples. (**D**) Western blots of WT, cGAS^{KO}, and STING^{KO} BMDMs mock infected or exposed to B31-A3 at an MOI of 20 for 9 h. Each lane represents a biological duplicate representative of three independent experiments. Nonspecific band is indicated by an asterisk (*). (**E**) WT BMDMs were cocultured with strain B31-A3 at MOI of 20 for 3 h on coverslips. Cells were fixed and stained with Abs against Borrelial OspA, autophagy marker p62, and mitochondrial heat shock protein 60 (HSP60); counterstained with DAPI; and subjected to confocal microscopy. Arrow indicates *B. burgdorferi* DNA stained with DAPI. Error bars in (A)–(C) represent ± SEM of triplicate biological samples. One-way ANOVA Tukey post hoc was used in (A)–(C) to determine significance. ***$p < 0.001$. ns, not significant.

ligands to induce IFN-I. Expressions of proinflammatory cytokine transcripts *Il6* and *Tnfa* were unchanged or modestly altered in STING^{KO}, MAVS^{KO}, and IFNAR^{KO} MEFs, demonstrating all MEF lines remained responsive to *B. burgdorferi* lipoprotein engagement of TLR2 during coincubation (Supplemental Fig. 2B). Moreover, qRT-PCR to detect internal levels of borrelial flagellar gene, *flaB*, within host cells revealed roughly equivalent levels of *flaB* among WT and mutant MEF lines (Supplemental Fig. 2C). This indicates that altered ISG expression in STING- and IFNAR-deficient cells is not due to changes in the ability of viable *B. burgdorferi* to associate with these MEFs.

cGAS–STING modulates inflammation during B. burgdorferi *infection in vivo*

To determine roles for the cGAS–STING pathway in borrelial dissemination, tissue colonization, and inflammation during mammalian infection, we monitored bioluminescent *B. burgdorferi*, ML23 pBBE22*luc*, in real time by in vivo imaging in C57BL/6 WT, cGAS^{KO}, and STING^{KO} mice (Fig. 4). Mice were injected with D-luciferin before imaging, and one mouse in each group was not injected to serve as a bioluminescence background control (Fig. 4A). The absence of cGAS or STING did not alter the kinetic dissemination of *B. burgdorferi* or the borrelial load as observed in the images and by quantitative analysis of bioluminescence emission (Fig. 4A, 4B). Outgrowth from infected tissues confirmed that all genotypes were colonized with viable *B. burgdorferi* 28 d postinfection (Fig. 4C). To investigate whether the cGAS–STING pathway impacts the development of arthritic phenotypes, we collected tibiotarsal joints from WT and cGAS^{KO} mice for histopathology. Consistent with prior reports (82), *B. burgdorferi* induced mild arthritis in WT C57BL/6J mice at 28 d postinfection (Supplemental Fig. 3A). Interestingly, H&E staining revealed that the joints of cGAS^{KO} mice exhibited reduced synovial papillary hyperplasia, immune cell infiltration, and overall joint pathology scores, suggesting a trend toward reduced inflammation at the 28-d time point (Supplemental Fig. 3B). These results suggest that the cGAS–STING pathway may contribute to the development of inflammation during mammalian infection without impacting the ability of *B. burgdorferi* to readily disseminate and colonize secondary tissues.

Discussion

B. burgdorferi elicits robust innate and adaptive immune responses that involve induction of both IFN-I (IFN-α and β) and IFN-II (IFN-γ) cytokines that drive expression of an overlapping family of ISGs (12, 31, 35, 83, 84). Synovial tissue from patients with postinfection Lyme arthritis expressed ISGs that are associated with both type I and type II IFNs (25, 35, 85). Ab-mediated IFNAR blockade results in a significant reduction in joint inflammation in mice (12), and the inhibition of IFN-γ delays sustained ISG expression and inflammation during *B. burgdorferi* infection (12, 86). A number of prior studies have focused on identifying the signaling mechanisms responsible for IFN-I and ISGs elicited by *B. burgdorferi*. Both in vitro and in vivo studies have demonstrated that TLR adaptors MyD88 and TRIF are not the primary contributors to IFN-I induction (12, 13, 22, 87–90). Specifically, in the absence of TLR2 or TLR5, innate immune receptors that sense lipoproteins or flagella of degraded *B. burgdorferi*, respectively, the induction of ISGs and joint swelling is similar to WT mice (12, 87–89). Studies using human cells have implicated nucleic acid–sensing, endosomal localized TLRs (TLR7, 8, and 9) as regulators of IFN-I induction in human PBMCs challenged with *B. burgdorferi* ex vivo (13, 18, 19, 90). However, TLR9 inhibition does not impair ISG induction in BMDMs exposed to *B. burgdorferi*, in contrast with PBMCs (19, 22, 85). Thus, it is likely that multiple innate immune pathways are responsible for IFN-I induction during *B. burgdorferi* infection. Differences in IFN-I and inflammatory responses across

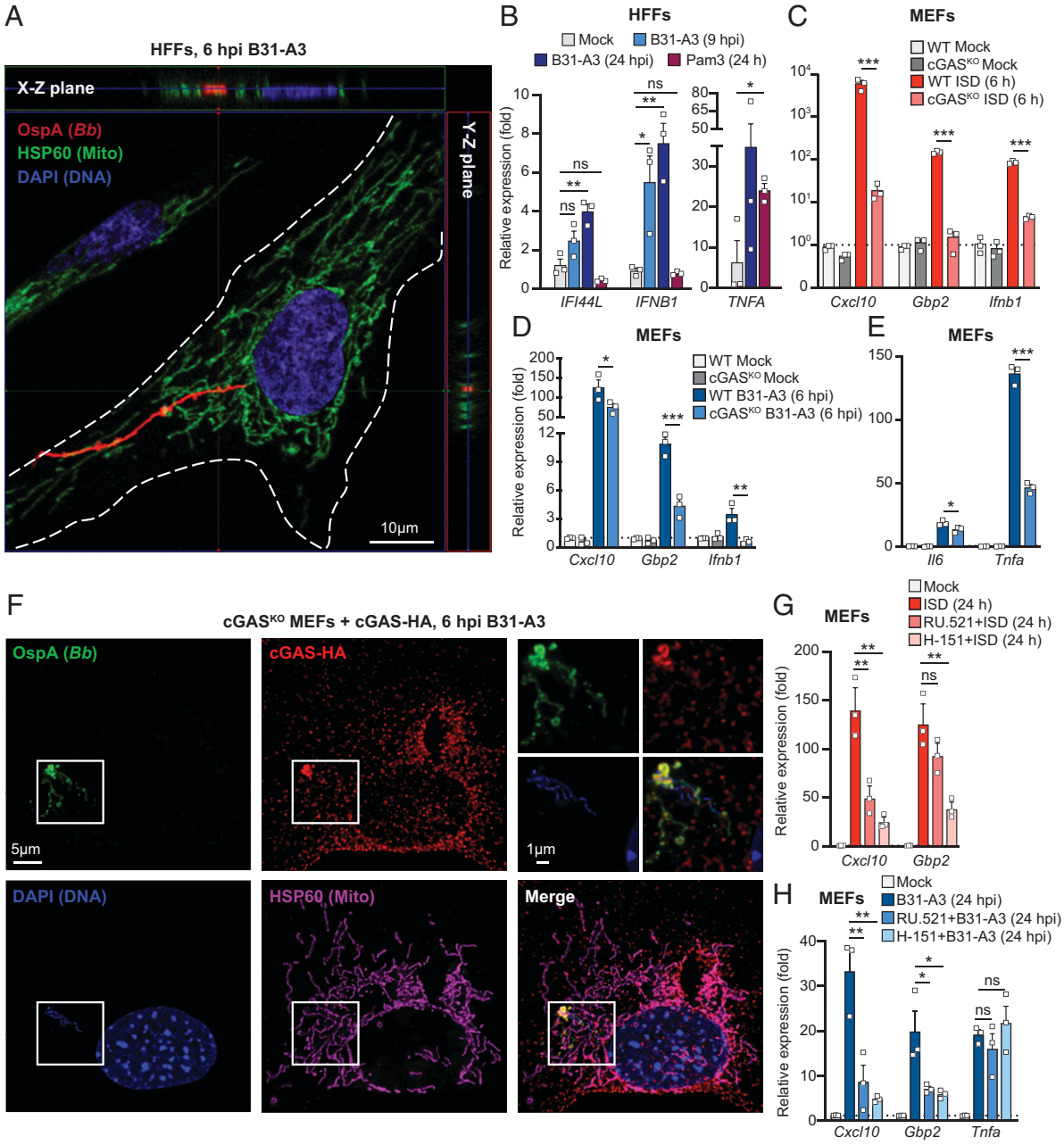

FIGURE 3. cGAS governs ISG expression in fibroblasts exposed to live *B. burgdorferi*. (**A** and **B**) Telomerase immortalized HFFs were cocultured with *B. burgdorferi* at an MOI of 20. (A) After 6 h of incubation, cells were fixed and stained with Abs against Borrelial OspA and mitochondrial heat shock protein 60 (HSP60), counterstained with DAPI, and subjected to confocal microscopy. Z-stack image reconstitution was performed to localize internalized *B. burgdorferi* with mitochondria. (B) After 9 and 24 h of coculture with B31-A3 or stimulation with the TLR ligand PAM3CSK4, RNA was extracted for qRT-PCR analysis of ISG (*IFI44L* and *IFNB1*) and inflammatory cytokine (*TNFA*) transcripts. (**C**) qRT-PCR of ISG (*Cxcl10*, *Gbp2*) and *Ifnb1* transcripts from WT and cGAS^{KO} MEFs 6 h after transfection with ISD or mock transfected. (**D** and **E**) qRT-PCR of transcripts encoding ISGs (*Cxcl10*, *Gbp2*) and *Ifnb1* (D) or inflammatory cytokines (*Il6* and *Tnfa*) (E) in WT and cGAS^{KO} MEFs exposed to live *B. burgdorferi* strain B31-A3 for 6 h at MOI of 20. (**F**) Immortalized cGAS^{KO} MEFs stably reconstituted with HA-tagged cGAS were cocultured with strain B31-A3 at MOI of 20 for 6 h on coverslips. Cells were fixed and stained with Abs against Borrelial OspA, HA (cGAS-HA), and mitochondrial HSP60, then counterstained with DAPI and subjected to fluorescence microscopy. (**G** and **H**) WT MEFs were treated with the cGAS inhibitor RU.512 or the STING inhibitor H-151 for 1 h before ISD transfection (G) or addition of *B. burgdorferi* B31-A3 (H). After 24 h of incubation, qRT-PCR analysis of ISG (*Cxcl10* and *Gbp2*) or inflammatory cytokine (*Tnfa*) transcripts was run. Fold expression values in (B)–(E), (G), and (H) are plotted relative to WT mock samples, and error bars represent ± SEM of triplicate biological samples. One-way ANOVA Tukey post hoc was used to determine significance. ***$p < 0.001$, **$p < 0.01$, *$p < 0.05$. ns, not significant.

independent studies might also be explained by the use of distinct borrelial strains that vary in invasion and inflammation (11, 91, 92).

Fibroblast and endothelial cells, which do not express a full complement of TLRs, are necessary for *B. burgdorferi*–induced IFN-I responses in joints (25, 41). Thus, TLR detection of *B. burgdorferi* nucleic acids is likely not the predominant pathway governing IFN-I responses during *B. burgdorferi* infection in the mammalian host. Therefore, we hypothesized that *B. burgdorferi* might engage an intracellular innate immune pathway leading to IFN-I. Using primary fibroblasts and macrophages from a panel of C57BL/6J

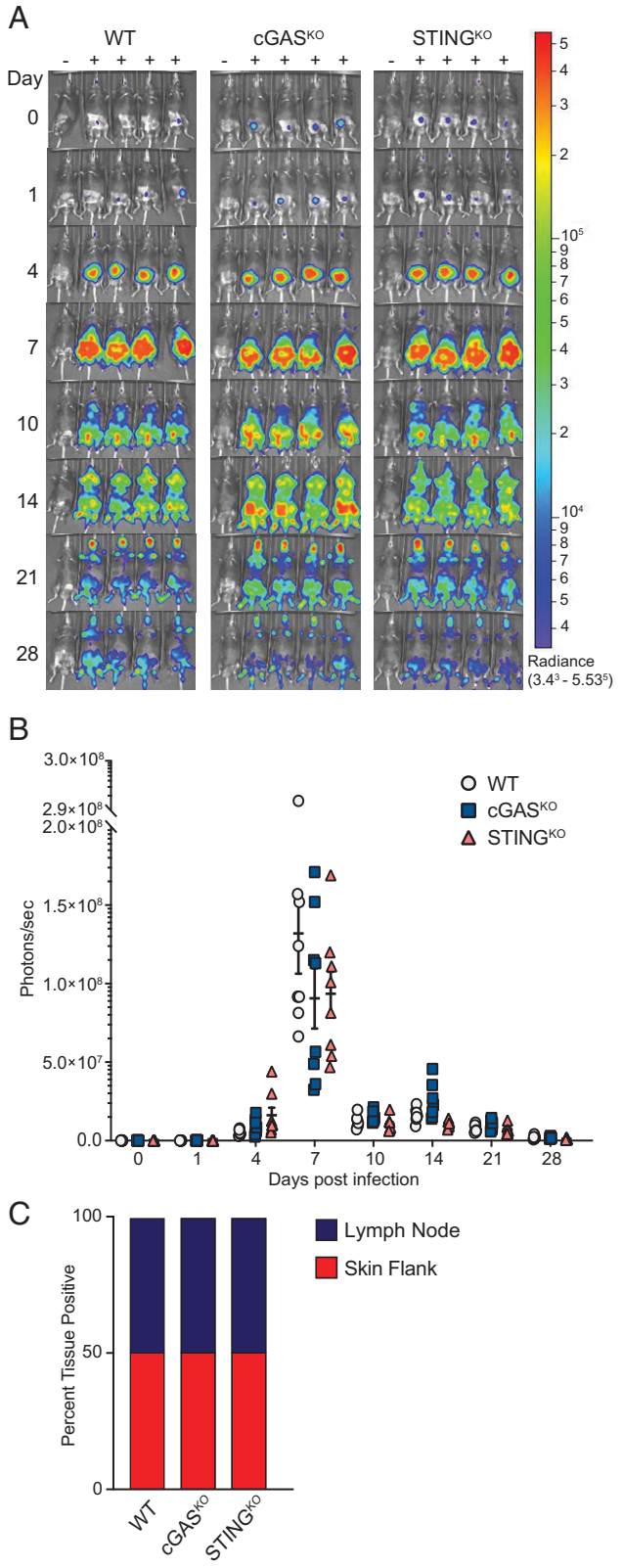

FIGURE 4. *B. burgdorferi* infection kinetics and tissue colonization are similar among WT, cGAS^{KO}, and STING^{KO} mice. WT, cGAS^{KO}, and STING^{KO} mice on the C57BL/6J background were infected with 10^5 ML23 pBBE22*luc* *B. burgdorferi* (n = 10/strain, 30 mice total). (**A**) Mice were selected randomly and treated with D-luciferin at 1, 4, 7, 10, 14, 21, and 28 d postinfection for in vivo imaging. For each mouse genotype, the mouse in the first column did not receive D-luciferin to serve as a background control. All images were normalized to the 3.4×10^3 to 5.53×10^5 radiance (p/s/cm^2/sr) and displayed on the same color spectrum scale (right). (**B**) Quantification of bioluminescence (in p/s). (**C**) Qualitative assessment of dissemination through tissue outgrowth. At day 28, five mice per strain were sacrificed after completion of imaging. An inguinal lymph node and skin flank were collected for in vitro cultivation. Percent of positive cultures is indicated by the *y*-axis. There was no significant difference in bioluminescence or tissue outgrowth across all mouse genotypes.

mice lacking intracellular nucleic acid sensors or downstream adaptors, we find that the DNA-sensing, cGAS–STING pathway is critically required for robust induction of ISGs after exposure to live *B. burgdorferi*. This finding was confirmed through small molecule inhibitor studies, because we observed reduced ISG responses to *B. burgdorferi* when cGAS or STING was inhibited in MEFs. In contrast, we show that deficiency of the main RIG-I–like receptor adaptor MAVS does not impact expression of ISGs or proinflammatory cytokine transcripts in fibroblasts, indicating that intracellular sensing of *B. burgdorferi* RNA is not a major contributor to IFN-I responses in cultured fibroblasts.

The phenomenon of host cell internalization by *B. burgdorferi* has not been observed during experimental infection in vivo; however, prior studies have shown that *B. burgdorferi* can become internalized into both phagocytic (macrophages, monocytes, and dendritic cells) and nonphagocytic (endothelial, fibroblast, and neuroglial cells) cells in culture (54, 57–62, 93–95). Our immunofluorescence microscopy analyses revealed borrelial OspA staining associated with a proportion of cultured mouse and human fibroblasts after short incubations with *B. burgdorferi* B31-A3. In both macrophages and fibroblasts, we observed OspA colocalization with the intracellular autophagy adaptor p62, which substantiates the notion that spirochetes interact with mammalian cells and can become internalized into the cytoplasm. Recent work has revealed that the autophagy machinery regulates the cGAS–STING pathway, because p62 is found in close proximity to TBK1, a key kinase necessary for IFN-I induction by STING (96). In addition, phosphorylation of p62 by TBK1 is important for the negative regulation and turnover of STING (97). Activation of cGAS by the obligate intracellular pathogen *Mycobacterium tuberculosis* can drive selective autophagy for clearance of intracellular bacteria (45). Interestingly, we observed coiled and degraded *B. burgdorferi* in BMDMs and MEFs colocalizing with p62, suggesting that the autophagy could be a mechanism to turn over internalized spirochetes. Autophagy has also been linked to inflammatory cytokine responses during *B. burgdorferi* infection in vitro (79). Therefore, internalization of *B. burgdorferi* and autophagic targeting may serve to fully engage intracellular signaling leading to IFN-I or other innate immune responses.

The cGAS–STING pathway is a major inducer of IFN-I in response to both exogenous, pathogen-derived DNA and host mtDNA and nuclear DNA (45, 51, 52, 72, 98–100). cGAS nondiscriminately binds dsDNA and produces 2′3′-cyclic guanosine monophosphate-adenosine monophosphate that binds and activates STING on the endoplasmic reticulum. This leads to recruitment and phosphorylation of the kinase TBK1, which phosphorylates and induces nuclear translocation of transcription factors IRF3 or IRF7 (101). Miller et al. (12) demonstrated that *B. burgdorferi* engages IFN-I response genes in an IRF3-dependent manner, further supporting that the signaling machinery downstream of cGAS–STING and other intracellular nucleic acid sensors is required for ISG induction. Multiple intracellular bacterial pathogens, including *Mycobacterium tuberculosis*, *Listeria monocytogenes*, and *Chlamydia trachomatis*, engage the cGAS–STING axis to induce IFN-I and influence pathogenesis (45, 50, 102–105). More recently, extracellular bacterial pathogens *Pseudomonas aeruginosa* and group B *Streptococcus* have been shown

to trigger IFN-I responses through cGAS–STING in macrophages and dendritic cells (52, 106). The mechanisms by which *B. burgdorferi* and other extracellular bacteria engage cGAS remain unclear. However, we have observed recruitment and colocalization of cGAS with intracellular borrelia in MEFs, suggesting that internalized spirochetes may shed DNA or undergo host-induced membrane damage that liberates bacterial genomic material for detection by cGAS. Bacterial pathogens can also cause host cell stress, resulting in the release and accumulation of nuclear or mtDNA (107, 108). Mitochondrial stress and mtDNA release, in particular, is linked to innate immune responses through the cGAS–STING axis and is associated with autoimmune disorders (i.e., lupus and rheumatoid arthritis) and other conditions characterized by elevated IFN-I (98). Thus, it is possible that the IFN-I response induced by *B. burgdorferi* is at least partially dependent on host mtDNA or nuclear DNA sensing. It is likely that *B. burgdorferi* engages distinct mechanisms in phagocytic and nonphagocytic cells to elicit IFN-I responses via the cGAS–STING pathway, and future work is required to reveal the molecular mechanisms involved.

An IFN-I response occurs early in mammalian infection, resulting in the development of inflammation and arthritis that persist in part because of IFN-γ during later stages of disease (32, 35, 83, 84). We therefore investigated how absence of cGAS and STING impacted the kinetics of borrelial infection in mice using in vivo imaging to track bioluminescent *B. burgdorferi* in real time through the progression of disease (70, 109). Bioluminescent *B. burgdorferi* was able to successfully disseminate and colonize secondary tissues independently of cGAS or STING. Joint inflammation also showed a moderate, although not statistically significant, reduction at 28 dpi in $cGAS^{KO}$ mice, suggesting that cGAS–STING signaling to IFN-I or other inflammatory response pathways might contribute to arthritic phenotypes during *B. burgdorferi* infection. It is important to note that the absence of cGAS did not eliminate inflammation entirely, indicating that *B. burgdorferi*–associated arthritis is multifactorial and involves additional innate and adaptive immune pathways as have been reported by others (13, 17, 19, 20, 90).

Although this study is impactful in that it is, to our knowledge, the first to link the cGAS–STING pathway to *B. burgdorferi*–induced IFN-I responses, it is not without limitations. C3H is the preferred model for borrelial infection because this background develops inflammation and pathologic disease at a significantly higher level than C57BL/6 or BALB/c mice (34, 82). An elegant study identified the *Bbaa1* locus in C3H mice is responsible for IFN-I responses observed during borrelial infection and showed that introduction of this locus into C57BL/6 mice yielded similar inflammatory responses to C3H (29). Our study employed WT, cGAS, and STING KO strains on a pure C57BL/6 background because they are commercially available and well characterized. We employed highly invasive and inflammatory RST1 *B. burgdorferi* B31-A3 for our studies and were able to observe IFN-I induction even in cells from the C57BL/6 background. These responses were markedly attenuated or lost when using sonicated *B. burgdorferi* B31-A3. Other studies have revealed weak or absent ISG expression during in vitro challenge with *B. burgdorferi*, although most used sonicated bacteria or less inflammatory RST3 strains (12, 22, 82, 87). This indicates that the C57BL/6 background is not devoid of IFN-I responsiveness to borrelial infection. Our work and previous studies show C57BL/6 mice and cell lines do produce measurable IFN-I and inflammatory responses to borrelial infection, and therefore we propose it is an appropriate model for this initial characterization of cGAS–STING in the innate immune response to *B. burgdorferi* (12). However, the development of cGAS or STING KO lines on the C3H background will be necessary to fully characterize the role of this innate immune pathway in *B. burgdorferi* infection dynamics, tissue-specific inflammation, and arthritic phenotypes in vivo.

In conclusion, to our knowledge, our study is the first to show that *B. burgdorferi* triggers the intracellular cGAS–STING DNA-sensing pathway to shape IFN-I responses in cultured cells. Future studies are needed to investigate the how borrelial cells initiate IFN-I responses through this pathway by characterizing the source of DNA that binds to cGAS (i.e., bacterial or host) and determining whether borrelial internalization is required. Loss of cGAS or STING does not appear to alter *B. burgdorferi* dissemination or its ability to colonize secondary tissues, but studies in C3H mice lacking this innate immune pathway may reveal differential bacterial kinetics and/or inflammatory responses that do impact the course of infection. Additional work to clarify these open questions may support the development cGAS- and/or STING-based immunotherapeutics that may be effective against active infection or persistent symptoms of *B. burgdorferi*, such as Lyme arthritis.

Acknowledgments

We thank members of the Hyde and West laboratories for helpful discussions. We thank Dr. Jon Skare for providing the OspA Ab. We thank Yuanjiu Lei for assistance preparing the visual abstract.

Disclosures

The authors have no financial conflicts of interest.

References

1. Steere, A. C., F. Strle, G. P. Wormser, L. T. Hu, J. A. Branda, J. W. R. Hovius, X. Li, and P. S. Mead. 2016. Lyme borreliosis. [Published erratum appears in 2017 *Nat. Rev. Dis. Primers* 3: 17062.] *Nat. Rev. Dis. Primers* 2: 16090.
2. Stanek, G., and F. Strle. 2018. Lyme borreliosis-from tick bite to diagnosis and treatment. *FEMS Microbiol. Rev.* 42: 233–258.
3. Radolf, J. D., M. J. Caimano, B. Stevenson, and L. T. Hu. 2012. Of ticks, mice and men: understanding the dual-host lifestyle of Lyme disease spirochaetes. *Nat. Rev. Microbiol.* 10: 87–99.
4. Shapiro, E. D. 2014. Lyme disease. *N. Engl. J. Med.* 371: 684.
5. Kugeler, K. J., A. M. Schwartz, M. J. Delorey, P. S. Mead, and A. F. Hinckley. 2021. Estimating the frequency of Lyme disease diagnoses, United States, 2010–2018. *Emerg. Infect. Dis.* 27: 616–619.
6. Mead, P. S. 2015. Epidemiology of Lyme disease. *Infect. Dis. Clin. North Am.* 29: 187–210.
7. Schwartz, A. M., A. F. Hinckley, P. S. Mead, S. A. Hook, and K. J. Kugeler. 2017. Surveillance for Lyme disease—United States, 2008-2015. *MMWR Surveill. Summ.* 66: 1–12.
8. Radolf, J. D., K. Strle, J. E. Lemieux, and F. Strle. 2021. Lyme disease in humans. *Curr. Issues Mol. Biol.* 42: 333–384.
9. Bamm, V. V., J. T. Ko, I. L. Mainprize, V. P. Sanderson, and M. K. B. Wills. 2019. Lyme disease frontiers: reconciling *Borrelia* biology and clinical conundrums. *Pathogens* 8: 299.
10. Khatchikian, C. E., R. B. Nadelman, J. Nowakowski, I. Schwartz, M. Z. Levy, D. Brisson, and G. P. Wormser. 2015. Public health impact of strain specific immunity to *Borrelia burgdorferi*. *BMC Infect. Dis.* 15: 472.
11. Strle, K., K. L. Jones, E. E. Drouin, X. Li, and A. C. Steere. 2011. *Borrelia burgdorferi* RST1 (OspC type A) genotype is associated with greater inflammation and more severe Lyme disease. *Am. J. Pathol.* 178: 2726–2739.
12. Miller, J. C., Y. Ma, J. Bian, K. C. F. Sheehan, J. F. Zachary, J. H. Weis, R. D. Schreiber, and J. J. Weis. 2008. A critical role for type I IFN in arthritis development following *Borrelia burgdorferi* infection of mice. *J. Immunol.* 181: 8492–8503.
13. Cervantes, J. L., S. M. Dunham-Ems, C. J. La Vake, M. M. Petzke, B. Sahay, T. J. Sellati, J. D. Radolf, and J. C. Salazar. 2011. Phagosomal signaling by *Borrelia burgdorferi* in human monocytes involves Toll-like receptor (TLR) 2 and TLR8 cooperativity and TLR8-mediated induction of IFN-beta. *Proc. Natl. Acad. Sci. USA* 108: 3683–3688.
14. Wooten, R. M., Y. Ma, R. A. Yoder, J. P. Brown, J. H. Weis, J. F. Zachary, C. J. Kirschning, and J. J. Weis. 2002. Toll-like receptor 2 plays a pivotal role in host defense and inflammatory response to *Borrelia burgdorferi*. *Vector Borne Zoonotic Dis.* 2: 275–278.
15. Marre, M. L., T. Petnicki-Ocwieja, A. S. DeFrancesco, C. T. Darcy, and L. T. Hu. 2010. Human integrin α(3)β(1) regulates TLR2 recognition of lipopeptides from endosomal compartments. *PLoS One* 5: e12871.
16. Dennis, V. A., S. Dixit, S. M. O'Brien, X. Alvarez, B. Pahar, and M. T. Philipp. 2009. Live *Borrelia burgdorferi* spirochetes elicit inflammatory mediators from human monocytes via the Toll-like receptor signaling pathway. *Infect. Immun.* 77: 1238–1245.

17. Shin, O. S., R. R. Isberg, S. Akira, S. Uematsu, A. K. Behera, and L. T. Hu. 2008. Distinct roles for MyD88 and Toll-like receptors 2, 5, and 9 in phagocytosis of *Borrelia burgdorferi* and cytokine induction. *Infect. Immun.* 76: 2341–2351.
18. Cervantes, J. L., C. J. La Vake, B. Weinerman, S. Luu, C. O'Connell, P. H. Verardi, and J. C. Salazar. 2013. Human TLR8 is activated upon recognition of *Borrelia burgdorferi* RNA in the phagosome of human monocytes. *J. Leukoc. Biol.* 94: 1231–1241.
19. Petzke, M. M., A. Brooks, M. A. Krupna, D. Mordue, and I. Schwartz. 2009. Recognition of *Borrelia burgdorferi*, the Lyme disease spirochete, by TLR7 and TLR9 induces a type I IFN response by human immune cells. *J. Immunol.* 183: 5279–5292.
20. Parthasarathy, G., and M. T. Philipp. 2018. Intracellular TLR7 is activated in human oligodendrocytes in response to *Borrelia burgdorferi* exposure. *Neurosci. Lett.* 671: 38–42.
21. Krupna-Gaylord, M. A., D. Liveris, A. C. Love, G. P. Wormser, I. Schwartz, and M. M. Petzke. 2014. Induction of type I and type III interferons by *Borrelia burgdorferi* correlates with pathogenesis and requires linear plasmid 36. *PLoS One* 9: e100174.
22. Miller, J. C., H. Maylor-Hagen, Y. Ma, J. H. Weis, and J. J. Weis. 2010. The Lyme disease spirochete *Borrelia burgdorferi* utilizes multiple ligands, including RNA, for interferon regulatory factor 3-dependent induction of type I interferon-responsive genes. *Infect. Immun.* 78: 3144–3153.
23. Hastey, C. J., J. Ochoa, K. J. Olsen, S. W. Barthold, and N. Baumgarth. 2014. MyD88- and TRIF-independent induction of type I interferon drives naive B cell accumulation but not loss of lymph node architecture in Lyme disease. *Infect. Immun.* 82: 1548–1558.
24. Salazar, J. C., S. Duhnam-Ems, C. La Vake, A. R. Cruz, M. W. Moore, M. J. Caimano, L. Velez-Climent, J. Shupe, W. Krueger, and J. D. Radolf. 2009. Activation of human monocytes by live *Borrelia burgdorferi* generates TLR2-dependent and -independent responses which include induction of IFN-beta. *PLoS Pathog.* 5: e1000444.
25. Lochhead, R. B., F. L. Sonderegger, Y. Ma, J. E. Brewster, D. Cornwall, H. Maylor-Hagen, J. C. Miller, J. F. Zachary, J. H. Weis, and J. J. Weis. 2012. Endothelial cells and fibroblasts amplify the arthritogenic type I IFN response in murine Lyme disease and are major sources of chemokines in *Borrelia burgdorferi*-infected joint tissue. *J. Immunol.* 189: 2488–2501.
26. Bernard, Q., M. Thakur, A. A. Smith, C. Kitsou, X. Yang, and U. Pal. 2019. *Borrelia burgdorferi* protein interactions critical for microbial persistence in mammals. *Cell. Microbiol.* 21: e12885.
27. Meddeb, M., W. Carpentier, N. Cagnard, S. Nadaud, A. Grillon, C. Barthel, S. J. De Martino, B. Jaulhac, N. Boulanger, and F. Schramm. 2016. Homogeneous inflammatory gene profiles induced in human dermal fibroblasts in response to the three main species of *Borrelia burgdorferi* sensu lato. *PLoS One* 11: e0164117.
28. Berner, A., M. Bachmann, J. Pfeilschifter, P. Kraiczy, and H. Mühl. 2015. Interferon-α curbs production of interleukin-22 by human peripheral blood mononuclear cells exposed to live *Borrelia burgdorferi*. *J. Cell. Mol. Med.* 19: 2507–2511.
29. Ma, Y., K. K. C. Bramwell, R. B. Lochhead, J. K. Paquette, J. F. Zachary, J. H. Weis, C. Teuscher, and J. J. Weis. 2014. *Borrelia burgdorferi* arthritis-associated locus *Bbaa1* regulates Lyme arthritis and K/B×N serum transfer arthritis through intrinsic control of type I IFN production. *J. Immunol.* 193: 6050–6060.
30. Jacek, E., B. A. Fallon, A. Chandra, M. K. Crow, G. P. Wormser, and A. Alaedini. 2013. Increased IFNα activity and differential antibody response in patients with a history of Lyme disease and persistent cognitive deficits. *J. Neuroimmunol.* 255: 85–91.
31. Marques, A., I. Schwartz, G. P. Wormser, Y. Wang, R. L. Hornung, C. Y. Demirkale, P. J. Munson, S.-P. Turk, C. Williams, C. R. Lee, et al. 2017. Transcriptome assessment of erythema migrans skin lesions in patients with early Lyme disease reveals predominant interferon signaling. *J. Infect. Dis.* 217: 158–167.
32. Petzke, M., and I. Schwartz. 2015. *Borrelia burgdorferi* pathogenesis and the immune response. *Clin. Lab. Med.* 35: 745–764.
33. Paquette, J. K., Y. Ma, C. Fisher, J. Li, S. B. Lee, J. F. Zachary, Y. S. Kim, C. Teuscher, and J. J. Weis. 2017. Genetic control of lyme arthritis by *Borrelia burgdorferi* arthritis-associated locus 1 is dependent on localized differential production of IFN-β and requires upregulation of myostatin. *J. Immunol.* 199: 3525–3534.
34. Barthold, S. W., D. S. Beck, G. M. Hansen, G. A. Terwilliger, and K. D. Moody. 1990. Lyme borreliosis in selected strains and ages of laboratory mice. *J. Infect. Dis.* 162: 133–138.
35. Lochhead, R. B., S. L. Arvikar, J. M. Aversa, R. I. Sadreyev, K. Strle, and A. C. Steere. 2019. Robust interferon signature and suppressed tissue repair gene expression in synovial tissue from patients with postinfectious, *Borrelia burgdorferi*-induced Lyme arthritis. *Cell. Microbiol.* 21: e12954.
36. Mason, L. M. K., A. Wagemakers, C. van 't Veer, A. Oei, W. J. van der Pot, K. Ahmed, T. van der Poll, T. B. H. Geijtenbeek, and J. W. R. Hovius. 2016. *Borrelia burgdorferi* induces TLR2-mediated migration of activated dendritic cells in an ex vivo human skin model. *PLoS One* 11: e0164040.
37. Oosting, M., H. Ter Hofstede, P. Sturm, G. J. Adema, B.-J. Kullberg, J. W. M. van der Meer, M. G. Netea, and L. A. B. Joosten. 2011. TLR1/TLR2 heterodimers play an important role in the recognition of *Borrelia* spirochetes. *PLoS One* 6: e25998.
38. Salazar, J. C., C. D. Pope, M. W. Moore, J. Pope, T. G. Kiely, and J. D. Radolf. 2005. Lipoprotein-dependent and -independent immune responses to spirochetal infection. *Clin. Diagn. Lab. Immunol.* 12: 949–958.
39. Barbalat, R., L. Lau, R. M. Locksley, and G. M. Barton. 2009. Toll-like receptor 2 on inflammatory monocytes induces type I interferon in response to viral but not bacterial ligands. *Nat. Immunol.* 10: 1200–1207.
40. Oosenbrug, T., M. J. van de Graaff, M. C. Haks, S. van Kasteren, and M. E. Ressing. 2020. An alternative model for type I interferon induction downstream of human TLR2. *J. Biol. Chem.* 295: 14325–14342.
41. Kawasaki, T., and T. Kawai. 2014. Toll-like receptor signaling pathways. *Front. Immunol.* 5: 461.
42. Cai, X., Y.-H. Chiu, and Z. J. Chen. 2014. The cGAS-cGAMP-STING pathway of cytosolic DNA sensing and signaling. *Mol. Cell* 54: 289–296.
43. Liu, S., X. Cai, J. Wu, Q. Cong, X. Chen, T. Li, F. Du, J. Ren, Y.-T. Wu, N. V. Grishin, and Z. J. Chen. 2015. Phosphorylation of innate immune adaptor proteins MAVS, STING, and TRIF induces IRF3 activation. *Science* 347: aaa2630.
44. Patrick, K. L., S. L. Bell, and R. O. Watson. 2016. For better or worse: cytosolic DNA sensing during intracellular bacterial infection induces potent innate immune responses. *J. Mol. Biol.* 428: 3372–3386.
45. Watson, R. O., S. L. Bell, D. A. MacDuff, J. M. Kimmey, E. J. Diner, J. Olivas, R. E. Vance, C. L. Stallings, H. W. Virgin, and J. S. Cox. 2015. The cytosolic sensor cGAS detects *Mycobacterium tuberculosis* DNA to induce type I interferons and activate autophagy. *Cell Host Microbe* 17: 811–819.
46. Gao, D., J. Wu, Y.-T. Wu, F. Du, C. Aroh, N. Yan, L. Sun, and Z. J. Chen. 2013. Cyclic GMP-AMP synthase is an innate immune sensor of HIV and other retroviruses. *Science* 341: 903–906.
47. Castanier, C., N. Zemirli, A. Portier, D. Garcin, N. Bidère, A. Vazquez, and D. Arnoult. 2012. MAVS ubiquitination by the E3 ligase TRIM25 and degradation by the proteasome is involved in type I interferon production after activation of the antiviral RIG-I-like receptors. *BMC Biol.* 10: 44.
48. Seth, R. B., L. Sun, C.-K. Ea, and Z. J. Chen. 2005. Identification and characterization of MAVS, a mitochondrial antiviral signaling protein that activates NF-kappaB and IRF 3. *Cell* 122: 669–682.
49. Kawai, T., K. Takahashi, S. Sato, C. Coban, H. Kumar, H. Kato, K. J. Ishii, O. Takeuchi, and S. Akira. 2005. IPS-1, an adaptor triggering RIG-I- and Mda5-mediated type I interferon induction. *Nat. Immunol.* 6: 981–988.
50. Hansen, K., T. Prabakaran, A. Laustsen, S. E. Jørgensen, S. H. Rahbæk, S. B. Jensen, R. Nielsen, J. H. Leber, T. Decker, K. A. Horan, et al. 2014. *Listeria monocytogenes* induces IFNβ expression through an IFI16-, cGAS- and STING-dependent pathway. *EMBO J.* 33: 1654–1666.
51. Liu, N., X. Pang, H. Zhang, and P. Ji. 2022. The cGAS–STING pathway in bacterial infection and bacterial immunity. *Front. Immunol.* 12: 814709.
52. Zhou, C. M., B. Wang, Q. Wu, P. Lin, S. G. Qin, Q. Q. Pu, X. J. Yu, and M. Wu. 2020. Identification of cGAS as an innate immune sensor of extracellular bacterium *Pseudomonas aeruginosa*. *iScience* 24: 101928.
53. Liu, H., P. Moura-Alves, G. Pei, H.-J. Mollenkopf, R. Hurwitz, X. Wu, F. Wang, S. Liu, M. Ma, Y. Fei, et al. 2019. cGAS facilitates sensing of extracellular cyclic dinucleotides to activate innate immunity. *EMBO Rep.* 20: e46293.
54. Wu, J., E. H. Weening, J. B. Faske, M. Höök, and J. T. Skare. 2011. Invasion of eukaryotic cells by *Borrelia burgdorferi* requires β(1) integrins and Src kinase activity. *Infect. Immun.* 79: 1338–1348.
55. Woitzik, P., and S. Linder. 2021. Molecular mechanisms of *Borrelia burgdorferi* phagocytosis and intracellular processing by human macrophages. *Biology (Basel)* 10: 567.
56. Carreras-González, A., D. Barriales, A. Palacios, M. Montesinos-Robledo, N. Navasa, M. Azkargorta, A. Peña-Cearra, J. Tomás-Cortázar, I. Escobes, M. A. Pascual-Itoiz, et al. 2019. Regulation of macrophage activity by surface receptors contained within *Borrelia burgdorferi*-enriched phagosomal fractions. *PLoS Pathog.* 15: e1008163.
57. Williams, S. K., Z. P. Weiner, and R. D. Gilmore. 2018. Human neuroglial cells internalize *Borrelia burgdorferi* by coiling phagocytosis mediated by Daam1. *PLoS One* 13: e0197413.
58. Killpack, T. L., M. Ballesteros, S. C. Bunnell, A. Bedugnis, L. Kobzik, L. T. Hu, and T. Petnicki-Ocwieja. 2017. Phagocytic receptors activate Syk and Src signaling during *Borrelia burgdorferi* phagocytosis. *Infect. Immun.* 85: e00004-17.
59. Petnicki-Ocwieja, T., and A. Kern. 2014. Mechanisms of *Borrelia burgdorferi* internalization and intracellular innate immune signaling. *Front. Cell. Infect. Microbiol.* 4: 175.
60. Cruz, A. R., M. W. Moore, C. J. La Vake, C. H. Eggers, J. C. Salazar, and J. D. Radolf. 2008. Phagocytosis of *Borrelia burgdorferi*, the Lyme disease spirochete, potentiates innate immune activation and induces apoptosis in human monocytes. *Infect. Immun.* 76: 56–70.
61. Livengood, J. A., and R. D. Gilmore, Jr. 2006. Invasion of human neuronal and glial cells by an infectious strain of *Borrelia burgdorferi*. [Published erratum appears in 2015 *Microbes Infect.* 17: e1.] *Microbes Infect.* 8: 2832–2840.
62. Ma, Y., A. Sturrock, and J. J. Weis. 1991. Intracellular localization of *Borrelia burgdorferi* within human endothelial cells. *Infect. Immun.* 59: 671–678.
63. Burdette, D. L., K. M. Monroe, K. Sotelo-Troha, J. S. Iwig, B. Eckert, M. Hyodo, Y. Hayakawa, and R. E. Vance. 2011. STING is a direct innate immune sensor of cyclic di-GMP. *Nature* 478: 515–518.
64. Rogers, E. A., D. Terekhova, H.-M. Zhang, K. M. Hovis, I. Schwartz, and R. T. Marconi. 2009. Rrp1, a cyclic-di-GMP-producing response regulator, is an important regulator of *Borrelia burgdorferi* core cellular functions. *Mol. Microbiol.* 71: 1551–1573.
65. Caimano, M. J., S. Dunham-Ems, A. M. Allard, M. B. Cassera, M. Kenedy, and J. D. Radolf. 2015. Cyclic di-GMP modulates gene expression in Lyme disease spirochetes at the tick-mammal interface to promote spirochete survival during the blood meal and tick-to-mammal transmission. *Infect. Immun.* 83: 3043–3060.
66. Savage, C. R., W. K. Arnold, A. Gjevre-Nail, B. J. Koestler, E. L. Bruger, J. R. Barker, C. M. Waters, and B. Stevenson. 2015. Intracellular concentrations of *Borrelia burgdorferi* cyclic di-AMP are not changed by altered expression of the CdaA synthase. *PLoS One* 10: e0125440.
67. Barbour, A. G. 1984. Isolation and cultivation of Lyme disease spirochetes. *Yale J. Biol. Med.* 57: 521–525.

68. Zückert, W. R. 2007. Laboratory maintenance of *Borrelia burgdorferi. Curr. Protoc. Microbiol.* 12: 12C.1.1–12C.1.10.
69. Labandeira-Rey, M., and J. T. Skare. 2001. Decreased infectivity in *Borrelia burgdorferi* strain B31 is associated with loss of linear plasmid 25 or 28-1. *Infect. Immun.* 69: 446–455.
70. Hyde, J. A., E. H. Weening, M. Chang, J. P. Trzeciakowski, M. Höök, J. D. Cirillo, and J. T. Skare. 2011. Bioluminescent imaging of *Borrelia burgdorferi* in vivo demonstrates that the fibronectin-binding protein BBK32 is required for optimal infectivity. *Mol. Microbiol.* 82: 99–113.
71. Elias, A. F., P. E. Stewart, D. Grimm, M. J. Caimano, C. H. Eggers, K. Tilly, J. L. Bono, D. R. Akins, J. D. Radolf, T. G. Schwan, and P. Rosa. 2002. Clonal polymorphism of *Borrelia burgdorferi* strain B31 MI: implications for mutagenesis in an infectious strain background. *Infect. Immun.* 70: 2139–2150.
72. West, A. P., W. Khoury-Hanold, M. Staron, M. C. Tal, C. M. Pineda, S. M. Lang, M. Bestwick, B. A. Duguay, N. Raimundo, D. A. MacDuff, et al. 2015. Mitochondrial DNA stress primes the antiviral innate immune response. *Nature* 520: 553–557.
73. Lei, Y., C. Guerra Martinez, S. Torres-Odio, S. L. Bell, C. E. Birdwell, J. D. Bryant, C. W. Tong, R. O. Watson, L. C. West, and A. P. West. 2021. Elevated type I interferon responses potentiate metabolic dysfunction, inflammation, and accelerated aging in mtDNA mutator mice. *Sci. Adv.* 7: eabe7548.
74. De Nardo, D., D. V. Kalvakolanu, and E. Latz. 2018. Immortalization of murine bone marrow-derived macrophages. *Methods Mol. Biol.* 1784: 35–49.
75. Yan, M., Y. Li, Q. Luo, W. Zeng, X. Shao, L. Li, Q. Wang, D. Wang, Y. Zhang, H. Diao, et al. 2022. Mitochondrial damage and activation of the cytosolic DNA sensor cGAS–STING pathway lead to cardiac pyroptosis and hypertrophy in diabetic cardiomyopathy mice. *Cell Death Discov.* 8: 258.
76. Haag, S. M., M. F. Gulen, L. Reymond, A. Gibelin, L. Abrami, A. Decout, M. Heymann, F. G. van der Goot, G. Turcatti, R. Behrendt, and A. Ablasser. 2018. Targeting STING with covalent small-molecule inhibitors. *Nature* 559: 269–273.
77. Torres-Odio, S., Y. Lei, S. Gispert, A. Maletzko, J. Key, S. S. Menissy, I. Wittig, G. Auburger, and A. P. West. 2021. Loss of mitochondrial protease CLPP activates type I IFN responses through the mitochondrial DNA-cGAS–STING signaling axis. *J. Immunol.* 206: 1890–1900.
78. Skare, J. T., D. K. Shaw, J. P. Trzeciakowski, and J. A. Hyde. 2016. In vivo imaging demonstrates that *Borrelia burgdorferi* ospC is uniquely expressed temporally and spatially throughout experimental infection. *PLoS One* 11: e0162501.
79. Buffen, K., M. Oosting, S. Mennens, P. K. Anand, T. S. Plantinga, P. Sturm, F. L. van de Veerdonk, J. W. M. van der Meer, R. J. Xavier, T.-D. Kanneganti, et al. 2013. Autophagy modulates *Borrelia burgdorferi*-induced production of interleukin-1β (IL-1β). *J. Biol. Chem.* 288: 8658–8666.
80. Buffen, K., M. Oosting, Y. Li, T.-D. Kanneganti, M. G. Netea, and L. A. B. Joosten. 2016. Autophagy suppresses host adaptive immune responses toward *Borrelia burgdorferi. J. Leukoc. Biol.* 100: 589–598.
81. Grijmans, B. J. M., S. B. van der Kooij, M. Varela, and A. H. Meijer. 2022. *LAPped in Proof:* LC3-associated phagocytosis and the arms race against bacterial pathogens. *Front. Cell. Infect. Microbiol.* 11: 809121.
82. Ma, Y., K. P. Seiler, E. J. Eichwald, J. H. Weis, C. Teuscher, and J. J. Weis. 1998. Distinct characteristics of resistance to *Borrelia burgdorferi*-induced arthritis in C57BL/6N mice. *Infect. Immun.* 66: 161–168.
83. Lochhead, R. B., D. Ordoñez, S. L. Arvikar, J. M. Aversa, L. S. Oh, B. Heyworth, R. Sadreyev, A. C. Steere, and K. Strle. 2019. Interferon-gamma production in Lyme arthritis synovial tissue promotes differentiation of fibroblast-like synoviocytes into immune effector cells. *Cell. Microbiol.* 21: e12992.
84. Petzke, M. M., R. Iyer, A. C. Love, Z. Spieler, A. Brooks, and I. Schwartz. 2016. *Borrelia burgdorferi* induces a type I interferon response during early stages of disseminated infection in mice. *BMC Microbiol.* 16: 29.
85. Shin, J. J., L. J. Glickstein, and A. C. Steere. 2007. High levels of inflammatory chemokines and cytokines in joint fluid and synovial tissue throughout the course of antibiotic-refractory lyme arthritis. *Arthritis Rheum.* 56: 1325–1335.
86. Brown, C. R., and S. L. Reiner. 1999. Genetic control of experimental lyme arthritis in the absence of specific immunity. *Infect. Immun.* 67: 1967–1973.
87. Bolz, D. D., R. S. Sundsbak, Y. Ma, S. Akira, C. J. Kirschning, J. F. Zachary, J. H. Weis, and J. J. Weis. 2004. MyD88 plays a unique role in host defense but not arthritis development in Lyme disease. *J. Immunol.* 173: 2003–2010.
88. Behera, A. K., E. Hildebrand, J. Szafranski, H.-H. Hung, A. J. Grodzinsky, R. Lafyatis, A. E. Koch, R. Kalish, G. Perides, A. C. Steere, and L. T. Hu. 2006. Role of aggrecanase 1 in Lyme arthritis. *Arthritis Rheum.* 54: 3319–3329.
89. Liu, N., R. R. Montgomery, S. W. Barthold, and L. K. Bockenstedt. 2004. Myeloid differentiation antigen 88 deficiency impairs pathogen clearance but does not alter inflammation in *Borrelia burgdorferi*-infected mice. *Infect. Immun.* 72: 3195–3203.
90. Love, A. C., I. Schwartz, and M. M. Petzke. 2014. *Borrelia burgdorferi* RNA induces type I and III interferons via Toll-like receptor 7 and contributes to production of NF-κB-dependent cytokines. *Infect. Immun.* 82: 2405–2416.
91. Jones, K. L., G. A. McHugh, L. J. Glickstein, and A. C. Steere. 2009. Analysis of *Borrelia burgdorferi* genotypes in patients with Lyme arthritis: high frequency of ribosomal RNA intergenic spacer type 1 strains in antibiotic-refractory arthritis. *Arthritis Rheum.* 60: 2174–2182.
92. Mason, L. M. K., E. A. Herkes, M. A. Krupna-Gaylord, A. Oei, T. van der Poll, G. P. Wormser, I. Schwartz, M. M. Petzke, and J. W. R. Hovius. 2015. *Borrelia burgdorferi* clinical isolates induce human innate immune responses that are not dependent on genotype. *Immunobiology* 220: 1141–1150.
93. Hawley, K., N. Navasa, C. M. Olson, Jr., T. C. Bates, R. Garg, M. N. Hedrick, D. Conze, M. Rincón, and J. Anguita. 2012. Macrophage p38 mitogen-activated protein kinase activity regulates invariant natural killer T-cell responses during *Borrelia burgdorferi* infection. *J. Infect. Dis.* 206: 283–291.
94. Filgueira, L., F. O. Nestlé, M. Rittig, H. I. Joller, and P. Groscurth. 1996. Human dendritic cells phagocytose and process *Borrelia burgdorferi. J. Immunol.* 157: 2998–3005.
95. Naj, X., A.-K. Hoffmann, M. Himmel, and S. Linder. 2013. The formins FMNL1 and mDia1 regulate coiling phagocytosis of *Borrelia burgdorferi* by primary human macrophages. *Infect. Immun.* 81: 1683–1695.
96. Zhang, K., S. Wang, H. Gou, J. Zhang, and C. Li. 2021. Crosstalk between autophagy and the cGAS–STING signaling pathway in type I interferon production. *Front. Cell Dev. Biol.* 9: 748485.
97. Prabakaran, T., C. Bodda, C. Krapp, B.-C. Zhang, M. H. Christensen, C. Sun, L. Reinert, Y. Cai, S. B. Jensen, M. K. Skouboe, et al. 2018. Attenuation of cGAS–STING signaling is mediated by a p62/SQSTM1-dependent autophagy pathway activated by TBK1. *EMBO J.* 37: e97858.
98. West, A. P., and G. S. Shadel. 2017. Mitochondrial DNA in innate immune responses and inflammatory pathology. *Nat. Rev. Immunol.* 17: 363–375.
99. Wang, H., C. Zang, M. Ren, M. Shang, Z. Wang, X. Peng, Q. Zhang, X. Wen, Z. Xi, and C. Zhou. 2020. Cellular uptake of extracellular nucleosomes induces innate immune responses by binding and activating cGMP-AMP synthase (cGAS). *Sci. Rep.* 10: 15385.
100. Choudhuri, S., and N. J. Garg. 2020. PARP1-cGAS-NF-κB pathway of proinflammatory macrophage activation by extracellular vesicles released during *Trypanosoma cruzi* infection and Chagas disease. *PLoS Pathog.* 16: e1008474.
101. Ablasser, A., and Z. J. Chen. 2019. cGAS in action: exspanding roles in immunity and inflammation. *Science* 363: eaat8657.
102. Zhang, Y., L. Yeruva, A. Marinov, D. Prantner, P. B. Wyrick, V. Lupashin, and U. M. Nagarajan. 2014. The DNA sensor, cyclic GMP-AMP synthase, is essential for induction of IFN-β during *Chlamydia trachomatis* infection. *J. Immunol.* 193: 2394–2404.
103. Nandakumar, R., R. Tschismarov, F. Meissner, T. Prabakaran, A. Krissanaprasit, E. Farahani, B.-C. Zhang, S. Assil, A. Martin, W. Bertrams, et al. 2019. Intracellular bacteria engage a STING-TBK1-MVB12b pathway to enable paracrine cGAS–STING signalling. *Nat. Microbiol.* 4: 701–713.
104. Webster, S. J., S. Brode, L. Ellis, T. J. Fitzmaurice, M. J. Elder, N. O. Gekara, P. Tourlomousis, C. Bryant, S. Clare, R. Chee, et al. 2017. Detection of a microbial metabolite by STING regulates inflammasome activation in response to *Chlamydia trachomatis* infection. *PLoS Pathog.* 13: e1006383.
105. Su, X., H. Xu, M. French, Y. Zhao, L. Tang, X.-D. Li, J. Chen, and G. Zhong. 2022. Evidence for cGAS–STING signaling in the female genital tract resistance to *Chlamydia trachomatis* infection. *Infect. Immun.* 90: e0067021.
106. Andrade, W. A., A. Firon, T. Schmidt, V. Hornung, K. A. Fitzgerald, E. A. Kurt-Jones, P. Trieu-Cuot, D. T. Golenbock, and P.-A. Kaminski. 2016. Group B *Streptococcus* degrades cyclic-di-AMP to modulate STING-dependent type I interferon production. *Cell Host Microbe* 20: 49–59.
107. Kausar, S., L. Yang, M. N. Abbas, X. Hu, Y. Zhao, Y. Zhu, and H. Cui. 2020. Mitochondrial DNA: a key regulator of anti-microbial innate immunity. *Genes (Basel)* 11: 86.
108. Gao, Y., W. Xu, X. Dou, H. Wang, X. Zhang, S. Yang, H. Liao, X. Hu, and H. Wang. 2019. Mitochondrial DNA leakage caused by *Streptococcus pneumoniae* hydrogen peroxide promotes type I IFN expression in lung cells. *Front. Microbiol.* 10: 630.
109. Hyde, J. A., and J. T. Skare. 2018. Detection of bioluminescent *Borrelia burgdorferi* from in vitro cultivation and during murine infection. *Methods Mol. Biol.* 1690: 241–257.